OPEN ACCESS

University of BRISTOL

Thompson, A. J., MacFarlane, J. R., Belnoue, J. P-H., & Hallett, S. R. (2020). Numerical modelling of compaction induced defects in thick 2D textile composites. *Materials and Design*, *196*, [109088]. https://doi.org/10.1016/j.matdes.2020.109088

University of Bristol - Explore Bristol Research
General rights

# Numerical modelling of compaction induced defects in thick 2D textile composites

Adam J. Thompson *, Joseph R. McFarlane, Jonathan P.-H. Belnoue, Stephen R. Hallett

Bristol Composite Institute (ACCIS), University of Bristol, Queen's Building, University Walk, Bristol BS8 1TR, UK

HIGHLIGHTS

- A novel method to simulate the compaction behaviour of textiles at the macroscopic scale is presented.
- The method is included into a conventional finite element approach for simulating the forming behaviour of textiles.
- The ability of the method to capture compaction induced wrinkles is highlighted through comparison to experimental results.
- The approach is used to assess the effect that design and manufacturing parameters have on the quality of the final composite.

GRAPHICAL ABSTRACT
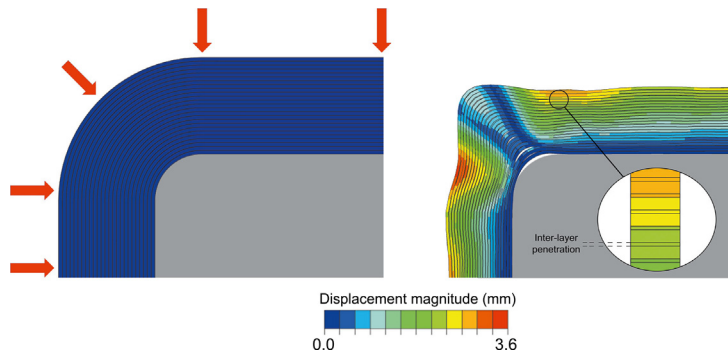
Displacement magnitude (mm)
0.0   3.6

ABSTRACT

This paper introduces a novel approach to include the high transverse compliance of textile materials into conventional forming simulations, allowing for the compaction process of thick 2D textile composites to be simulated. With this approach, the textile is presented as a continuous material using mutually constrained shell and membrane elements, this allows for both the high tensile stiffness and low out-of-plane bending stiffness to be present within the model. To include the through-thickness behaviour of the material, a compliant penalty contact is introduced which is able to capture the mechanical response of the material under compaction. By simulating the interaction between individual plies, the model is able to predict compaction induced wrinkle formation. The approach is used here to analyse the deformation behaviour of stacked layers compacted on to a male box tool to produce a C-section bracket. The model is validated against experimental results and used to assess the influence of key design and manufacturing parameters on defect formation.

© 2020 The Author(s). Published by Elsevier Ltd. This is an open access article under the CC BY license (http://creativecommons.org/licenses/by/4.0/).

1. Introduction

A key factor in the performance of composite structures is the quality of the final manufactured part. Regardless of the material form or process there are two common steps to produce components; the forming of an initially planar material into a three-dimensional shape and the compaction of the material to achieve the required thickness and fibre volume fraction. The deformation of a textile to accommodate forming and compaction processes is therefore an important attribute of the material which is dependent on both the material behaviour and the application of external pressure. Although these deformations are expected, their presence needs to be considered in the design process to ensure the final part conforms to requirements, and to minimise the occurrence of possible defects.

Defects can be categorised as irregularities in a structure or material causing the part to deviate from its intended design specification. Typically these irregularities are a result of the manufacturing process or are

* Corresponding author.
E-mail address: adam.thompson@bristol.ac.uk (A.J. Thompson).

a consequence of unrealistic design constraints. Potter [1] proposed a taxonomy of defects, highlighting the large variation of causes and the mechanisms leading to fibre path defects. This work highlighted that defects can be introduced in every stage of the manufacturing process, showing the importance for developing robust process simulation tools for each step in composite component production.

Out-of-plane defects, such as wrinkles and folds, have been recognised as one of the more severe defects and can significantly compromise the mechanical performance of composites. Potter et al. [2] reported a strength reduction of as much as 70% in four point bend tests when wrinkles were present. Similarly, Mukhopadyhyay et al. [3,4] studied the effect of embedded wrinkles on the tensile and compressive failure of unidirectional composite laminates. The presence of wrinkles was observed to reduce the tensile strength by more than 20% and a reduction of up to 30% was reported in the compressive strength.

In both studies by Mukhopadyhyay et al. finite element models, replicating the defected parts, were built directly from micrographs in order to understand, precisely, the failure mechanisms induced by the presence of the defect. Varkonyi et al. [5] used manufacturing process simulation to predict the 'as-manufactured' fibre paths to be used in mechanical performance models. It was shown that the predicted 'as-manufactured' models were significantly more accurate than pristine 'as-designed' models, reducing the error by up to 50% in parts where defects were present. This demonstrates the potential benefits that process simulation has in the design and manufacture of composite components. The ability to predict such defects and then include them in structural simulations serves as a powerful tool to optimise the design and the manufacturing process as defects and their knock down on performance can be identified prior to manufacture.

For textiles, the development of modelling techniques to predict their behaviour during the forming process in composite manufacture is a mature research topic. Models are now capable of including a large range of complex behaviours from in-plane bending stiffness [6,7], which resists abrupt changes in fibre directions, out-of-plane bending stiffness [8,9], key for capturing the formation, shape and size of out-of-plane wrinkles, to shear-tension coupling [10] and more recently the irreversibility of some of these behaviours [11]. In these methods, the high through-thickness compliance of the material is often neglected, which is a reasonable assumption when considering just a single layer of material, as the deformations are dominated by large in-plane shear and out-of-plane bending. However, when multiple layers of material are stacked to create a thicker component, the change in thickness, due to compaction, accumulates and can become a significant mode of deformation that can produce severe defects in curved and complex geometries [12].

To date, research into the compaction behaviour of textiles has largely focused on the deformation of its internal architecture and its non-linear mechanical response as a result of that loading [13–15]. The macro-scale compaction behaviour has received little attention as the magnitude of deformation is often superseded by that caused during the forming process. Research into compaction induced defects, such as wrinkles, has therefore revolved mainly around uni-directional prepregs, with mechanisms behind their formation and models to predict their occurrence being presented [12,16–22].

In this paper, a new modelling approach is introduced that allows for the through-thickness compliance of textile materials to be included into conventional forming simulations, using shell and membrane finite elements. Implemented into the commercially available finite element software, Abaqus/Explicit, the method allows for the high stiffness of the fibre direction, non-linear shear stiffness, out-of-plane bending stiffness and through-thickness compressibility of textiles to be present within the model. The model is used to simulate the compaction of large numbers of textile layers, typical for thick composites components, over singly curved tooling. The ability of the method to predict defects is first shown through comparison with experimental results,

the model is then used to assess the influence that design and manufacturing parameters have on the formation of defects.

2. Mechanism of compaction induced defects

During the compaction of fibrous materials gaps between the individual fibres are closed and the fibres are forced to rearrange through sliding and bending, providing little resistance to the external pressure. As the fibres come into contact, and the number of contacts increase, rapid stiffening occurs until the inter-fibre contacts fully constrain the fibrous network [23]. Although this results in a highly compliant material with a non-linear stiffness response, the thickness of a single layer of 2D woven fabrics is very small (« 1 mm) and hence, at the macroscopic scale, the change in thickness can often be assumed to be negligible. However, when multiple layers are introduced to produce thick components, the change in thickness accumulates and can become significant.

The change in thickness can be problematic for the case where multiple layers are compacted over three dimensional surfaces. In this instance, the large change in thickness leads to a change in path length of each layer of material. For male radii, the path length is reduced, which leads to the accumulation of excess material, while for female radii, the change in thickness leads to insufficient material to cover the final surface.

If the layers are able to slide with respect to one another then, for male radii, the excess length is pushed to the edge of the part, for female radii, material is pulled towards the radius. In both instances, this migration of material causes the so called 'book ending' at the edge of the part [12]. If the layers are, however, unable to slide because of high friction forces or geometric features, then the material must deform to accommodate it. The mechanism by which the material will deform will be that which requires the least energy. Bridging is commonly observed in female radii while for male radii, buckling of the fibres is typical. The fibre buckling can occur either in-plane or out-of-plane and is affected by fibre direction, tool geometry and pressure distribution [24].

For compaction over male radii, the excess length, resulting from the change in thickness, can be calculated using Eq. (1). The change in thickness, Δt, is the only physical parameter which affects the quantity of excess length, with L_{ex} increasing with increasing magnitudes of Δt.

$$L_{ex} = \frac{2\pi\Delta t}{4} \tag{1}$$

3. Numerical approach

The way by which excess length is accommodated is dependent on the material behaviour and the constraints enforced by geometric features. Simulating this phenomenon, therefore, necessitates including not only the through-thickness compliance of the material into a model, but also the other characteristic material behaviours typically included in forming simulations i.e. high stiffness along fibre directions, in-plane shear behaviour and out-of-plane bending stiffness.

3.1. Forming model

The foundation of this approach is based on the forming approach presented in [25] where and individual fabric layers are represented as continuous planar materials and the mechanical behaviour of the mesoscopic scale is considered through constitutive models. The method uses a continuum hypoelastic material model within Abaqus/Explicit, which has been successfully used in a number of works [26–28]. The hypoelastic material model has been implemented as a user material subroutine (VUMAT) and is used to track the non-orthogonal change in yarn orientations during shear deformations and to calculate the fabric response from the tensile modulus along each of the fibre directions, E_1 and E_2, as well as the non-linear in-plane shear

response, G_{12}. Full details of the theory and its implementation can be found in [25] and the VUMAT is distributed for free from the Bristol Composite Institute (ACCIS) Github page (https://accis.github.io/HypoDrape/).

To include both the high tensile stiffness of the yarns and their significantly lower bending stiffness in the model, both shell and membrane elements are used. These are superimposed, sharing the same nodes so that the two elements are mutually constrained. The in-plane behaviour is controlled by the membrane element and the out-of-plane behaviour (i.e bending) is controlled by the shell element. The hypoelastic user-material subroutine is assigned to both element types. The membrane elements are prescribed with the in-plane material properties; tensile stiffness along the fibre directions and the non-linear shear stiffness. The shell elements, conversely, are assigned with a tensile modulus that is equivalent to the flexural modulus of the material, this is derived from the textile's bending rigidity obtained from a simple cantilever bending test. The shear rigidity of the shell elements is set to zero and so the fabric shear is controlled solely by the mutually constrained membrane elements. By coupling the behaviour of these two element types, the high tensile stiffness of the fabric is fully separated from its significantly lower bending stiffness. The use of the hypoelastic material model for the shell elements, as well as the membrane elements, assumes that the bending stiffness is projected along the fibre direction and rotates during shear deformation. This results in an anisotropic bending response that evolves with any shear transformations. This approach has been successful at modelling the forming of textiles over complex geometries, accurately capturing both the shear and wrinkle deformations as well as the interaction of multiple layers [25].

3.2. Including through thickness compression

A limitation of both shell and membrane elements, is that they have no through-thickness compliance. This prevents them from modelling the compaction of woven materials. Solid-shell elements, which allow for through thickness deformations, have recently seen substantial development and offer a promising solution to the problem [20,29]. These bespoke elements are, however, not available in commercial finite element solvers and user defined elements are often challenging to implement within them. An alternative approach is proposed here whereby the compressibility of the material is accounted for at the interface between adjacent layers through the introduction of a compliant penalty contact. One of the keys benefits of this is that the compressibility of the material requires no extra computation in the model, as ply level modelling always requires contact to be realised between adjacent plies.

The penalty contact method is a common contact formulation used in finite element analysis. This method introduces a force at contact detection points which have penetrated through a defined surface. The purpose of this force is to eliminate the penetration by pushing the two surfaces out of contact. The method uses the simple formula presented in Eq. (2).

$$F_c = k_c D_p \tag{2}$$

where k_c is the contact stiffness, often referred to as the penalty stiffness, and D_p is the depth of the penetration. The magnitude of the force required to remove the penetration is typically unknown, consequently there is often a finite amount of penetration at the end of each time step. The value of k_c is a fictional stiffness which must be large enough to minimise the penetration without being so large as to cause instability, and is the contact pressure between two surfaces as a function of the overclosure (depth of the penetration). Through manipulation of this relationship, the non-linear through-thickness compliance of the woven material can be included in the forming simulations as interpenetration between elements of adjacent layers. Including the through
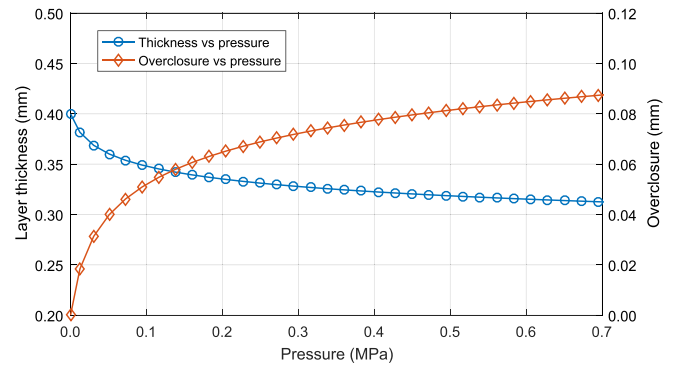

Fig. 1. Thickness-pressure response for a single layer of the plain woven fabric and the it's derived pressure-overclosure relationship.

thickness compliance of the material in this way relies on three key assumptions. Firstly, it is assumed that the compaction behaviour is fully uncoupled from the membrane and bending behaviour of the material, secondly, the through-thickness intra-ply shear is negligible and finally, it is assumed that the compression behaviour is fully reversible.

Fig. 1 shows the pressure-overclosure relationship for a single layer of carbon fibre plain woven fabric. This relationship was derived from compaction test of a single layer of the plain woven fabric between two rigid plates, where the overclosure is considered as the change in material thickness and the contact pressure is the externally applied pressure.

4. Verification of through-thickness behaviour

To verify the compliant penalty contact, a stack of 2D elements was modelled under transverse compression with the pressure overclosure relationship presented in Fig. 1 applied to the contact formulation between them. Single, square shell elements were stacked in a column, each element representing a layer of material and given a thickness of 0.4 mm. An in-plane displacement boundary condition was applied to all of the stacked elements to constrain their displacements to only vertical translations. The stacks were placed on a rigid surface with a fully fixed boundary condition. The pressure-overclosure relationship shown in Fig. 1 was applied to the general contact definition in tabular form. As this relationship is for a single layer compacted between two rigid plates, the model does not consider the nesting of the plies when stacked and, subsequently, its effect on the compaction response is not included. Nesting could be considered by using the compaction behaviour of multiple plies which can be found experimentally or via lower scale models [14,15].

Three tests were performed to verify the approach, each with a different number of layers. A schematic of the verification model for two layers is presented in Fig. 2. Fig. 3 shows each of the models before and after compaction. As previously explained, the reduction in thickness is achieved through inter-penetrations of contacting elements. The thickness-pressure response of each model is shown in Fig. 4. The model with just two layers matches well with the expected values, however, as the number of layers is increased the models become more compliant and diverge slightly from the input values. This is likely due to the build up of small numerical errors which increase with the number of layers, though the difference between 6 and 24 layers is less than observed between 2 and 6 layers suggesting that the error reaches a plateau.

5. Experiments of compaction induced wrinkles on curved tooling

Experiments were performed to examine compaction induced wrinkles as well as to provide a baseline validation case for the numerical study.
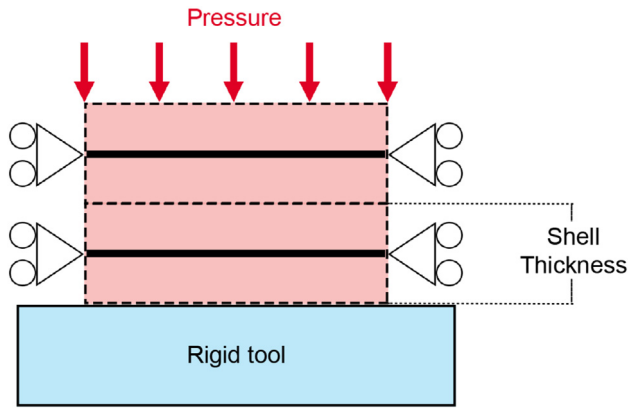
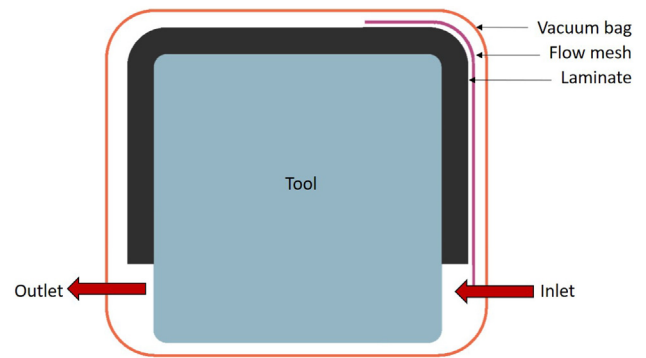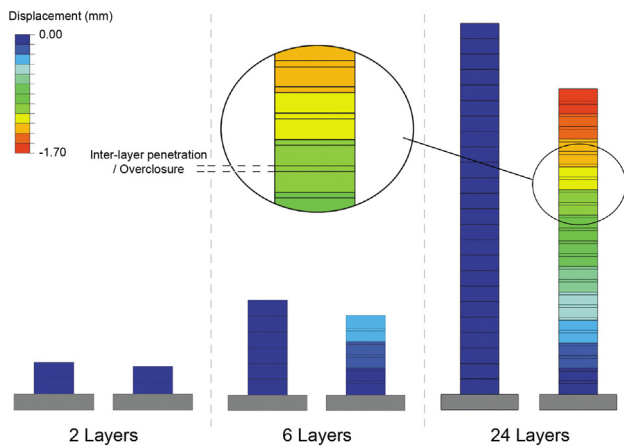**Fig. 2.** Schematic of the consolidation model verification study for two layers.

Fig. 3. Verification of compliant contact - pre and post-compacted models.

5.1. Material and lay-up

The material used was a balanced carbon fibre, plain woven fabric with 6 k tows and areal weight of 320 gsm. Each layer was aligned either 0°, or 45° to the radius of the tool, depending on its position within the stack. A total of 24 layers were used with a lay-up of $[0/90° \pm45°]_{12s}$. Following the compaction of the lay-up, Prime 20LV resin was used to infuse and fixate it, ready for sectioning.

Fig. 5. Schematic of bagging process for experiment defect samples.

5.2. Procedure

The individual layers were placed sequentially on to a 110 mm square box section tool with 5 mm corner radii and length of 300 mm. Flow mesh was placed on the surface of the lay-up, going around one of the radii. The second radius was left free of mesh, to reduce any influence it might have had on the development of defects in this region. The tool was then enveloped in a vacuum bag, with effort given to make it conform to the surface of the pre-compacted lay-up. A schematic of the manufacturing set up is shown in Fig. 5.

Vacuum was applied, and, once full vacuum was achieved, resin was released and drawn through the part at room temperature. Following cure, the part was sectioned, polished and scanned in a high definition flat-bed scanner. To quantify the results, images of three sections, taken from the centre of the part at 30 mm intervals, were post processed to find the relative thickness of the part at discrete locations around the profile of the tool.

5.3. Experimental results

An image showing one of the three cross-sections is presented in Fig. 6. A wrinkle appears in both radii, introduced through the compaction of the lay-up. The radius where the flow mesh was present has a less pronounced wrinkle, suggesting that the flow mesh affects its morphology. This can be seen more clearly in Fig. 7 which shows the thickness variation of the part at discrete locations. At the radius where no flow mesh was present, a wrinkle is observed in the second layer (Fig. 6), propagating and increasing in magnitude to the surface of the lay-up. It is clear that the excess length, produced by compacting multiple layers over a male
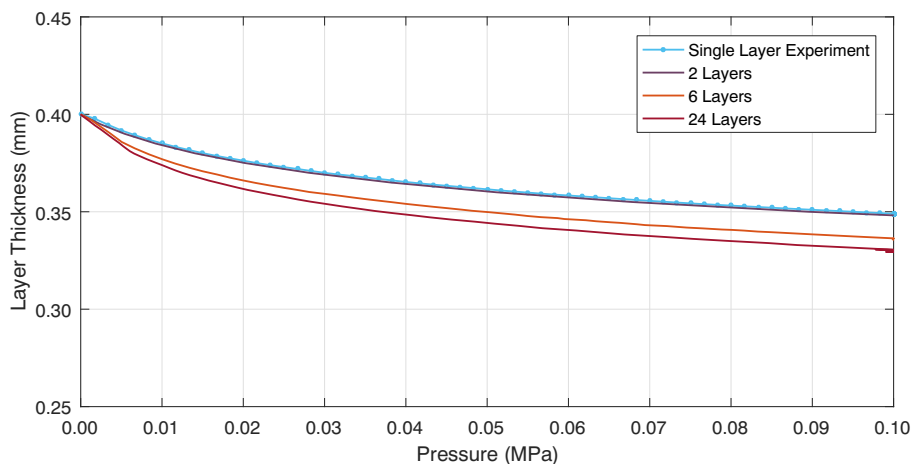

Fig. 4. Mechanical out-put of compliant contact verification study showing the normalised Thickness-Pressure relationship for each model.
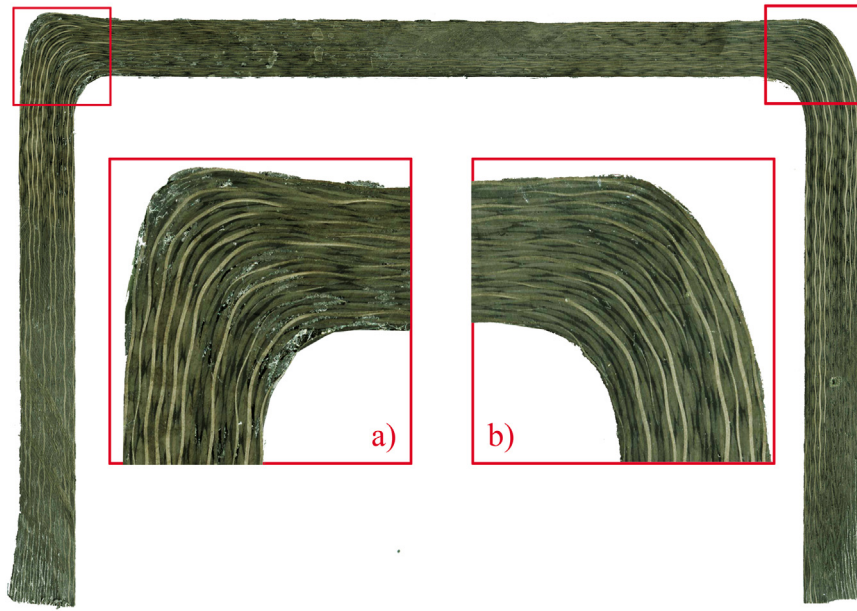
Fig. 6. Cross-section of C-section sample a) radius without flow mesh b) radius in contact with flow mesh.

radius, is confined to the region of the radius and caused the fibres to buckle out-of-plane, resulting in severe fibre misalignment.

6. Simulating the compaction of multiple layers over curved tooling

To assess the capability of the proposed model to capture consolidation-induced defects, simulations of the experimental case, described in Section 5, were performed.

As a prismatic tool, with only single curvature, was used in the experiments, the models were built under the assumption that the forming of the layers, to their pre-compacted position, caused no deviation of fibre angle and formed perfectly to the tool. The properties of the plain woven fabric required for the model are presented in Table 1. The non-linear shear behaviour of the textile, G_{12}, was derived from picture frame shear experiments on the plain weave fabric. A polynomial regression curve is fitted to this which describes the shear stiffness as a function of the shear angle, γ. The flexural stiffness applied to the shell elements was measured by performing a cantilever bending test on the material.

Table 1
Material input parameters for the respective elements in plain woven fabric model.

Element type	E_1 (MPa)	E_2 (MPa)	G_{12} (MPa)
Membrane	40,000	40,000	$32.37\gamma^4 - 59.31\gamma^3 + 36.36\gamma^2$ $- 7.394\gamma + 0.4576$
Shell	62	62	0

For simplicity, the tensile stiffness along the fibre direction was assumed to be linear and was calculated under the assumption that the fabric was perfectly balanced, the crimp is negligible and the as-woven geometry had a fibre volume fraction of 0.4. Coulomb friction was used to model the tangential interactions between layers, with a coefficient of 0.28, this value was taken from experimental results of the frictional interactions between layers of a plain woven carbon fibre fabric in [30].

Only the radius of the part where no flow mesh was present on the surface of the lay-up was considered. Symmetry boundary conditions were applied along the centre of the web, which means that the case
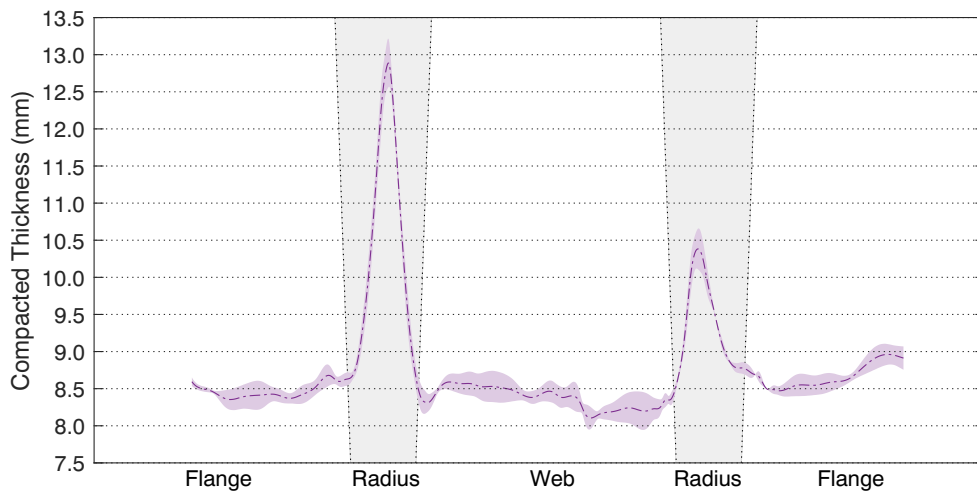

Fig. 7. Average thickness of three separate c-section specimens and the standard deviation.
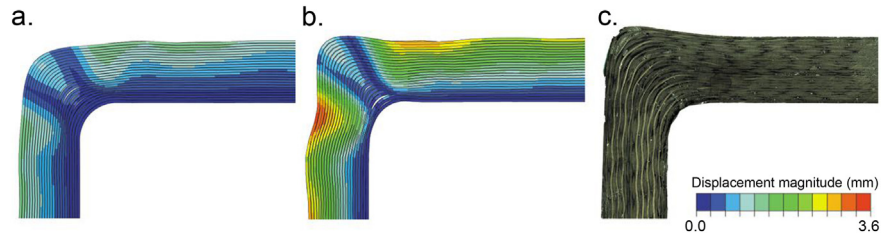
Fig. 8. Detail of wrinkle in radius a) simulation with perfect contact between plies b) simulation with 12.5% extra bulk included in the lay-up c) experiment.

with flow mesh was not considered as part of this numerical study. The bag was modelled as a linear elastic material using membrane elements, with a Young's Modulus of 2.6 GPa and Poisson's ratio of 0.4. As an envelope vacuum bag was used and conformed to the surface of the tool, it is reasonable to assume that it did not slip relative to the tool, therefore the extremities of the bag were constrained so that they could only move radially to the tool. A ramped pressure load of 0.1 MPa was applied to the surface of the bag to simulate the evacuation of air from within.

Two models were prepared, one where the layers were in perfect contact and conformed to the tool with a constant total thickness of 9.6 mm (0.4 mm × 24 layers) and a second model where a small gap of 0.05 mm was introduced between plies, producing 12.5% extra bulk to the lay-up.

Figs. 8 and 9 show the predictions of the model compared with the experiments. The simulation is able to capture the mechanisms responsible for the wrinkle and is able to reproduce a good representation of the experimental result, for both location and shape of the wrinkle. The model in which more bulk was introduced gives a good description of the size of the wrinkle, whereas the model with no bulk is more conservative, this can be attributed to the fact that perfect contact between layers is unlikely to be achieved during the lay-up procedure, with the flexural stiffness of the material creating small separations between the layers around the radius.

7. Design parameters influence on defect formation and severity

In this section, the model is used to examine the effect that various parameters, based on design and manufacturing choices, have on the formation and severity of the wrinkle. Four parameters are assessed:

- Pressure application.
- Fibre orientation.
- Tool radius.
- Arm length.

The model of the C-section described in Section 5, which produced wrinkles in both the experimental and numerical investigation, is

used. Each parameter is assessed independently and is compared with the baseline model, where no added bulk was introduced. In every model, 24 layers of the plain woven fabric are considered, each prescribed with the properties presented in Table 1. In all cases an external pressure of 0.1 MPa was applied to compact the lay-up.

7.1. Pressure distribution

With out-of-autoclave processes the sole source of compressive force on the material is from atmospheric pressure as the air is evacuated from within. The configuration of the vacuum bag, therefore, can have a significant effect on the distribution of pressure on the laminate. The experimental study presented in Section 5 used an envelope bag which naturally followed the surface of the laminate, this results in excess length in the bag during the compaction process, consequently reducing pressure at the tool radii. If there is insufficient bagging material available to cover the geometry of the tool, through, for example, bag bridging at a female radius, the pressure over the male corners can be greater than the applied pressure, due to membrane forces in the bag.

In this study, three different pressure distributions are compared. Firstly, the experimental case, where the bag naturally follows the surface of the laminate. The second model considers the case where there is insufficient bagging material, causing membrane stresses in the bag. The final model considers hydrostatic pressure exerted on the top layer of the laminate, with no vacuum bag modelled. The boundary conditions applied to each of the models are illustrated in Fig. 10.

Gradient plots of the thickness of the laminate around the tool are shown in Fig. 11 and the average thickness at discrete points around the tool profile are shown in 12a. Although the same magnitude of pressure was applied to compact the structure, the boundary conditions strongly effects the topology of the final structure.

The first model (baseline case) shows large thickening around the radius, due to a reduction in pressure at this region, whereas the second shows thinning in the corner region, this is induced through higher pressure being present at the radius due to membrane loading of the bag, pushing the excess length out of the laminate, through book ending. This membrane loading also appears to increase the thickness in
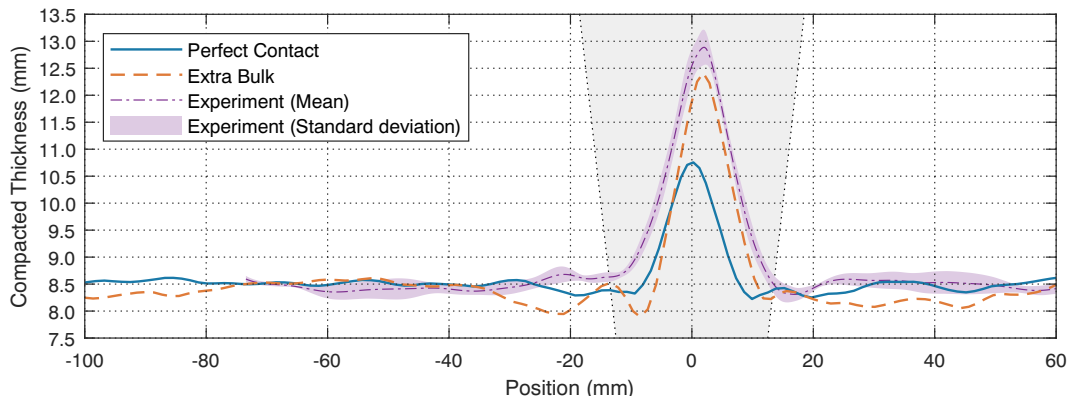

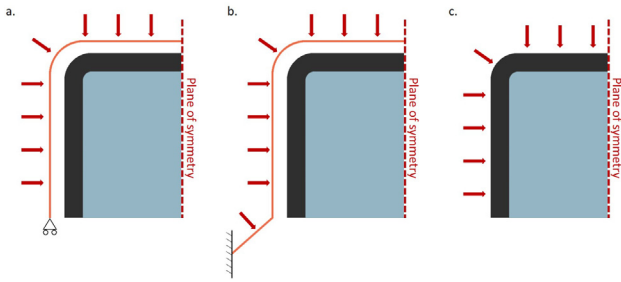**Fig. 9.** Thickness variation - comparison of simulation with experiment.

Fig. 10. Boundary conditions applied for pressure distribution study a) Conforming bag (baseline case) b) Bridging bag c) Hydrostatic pressure.

the flange as the bag bridging ensures the pressure is not applied normal to the tool surface. In the hydro-static case, a wrinkle at the corner region is observed, however, its shape is different to that of the baseline case as there is an even pressure being applied all the way around the radius, flattening the wrinkle out.

7.2. Fibre orientation

To assess the effect that fibre orientation has on the compacted laminate, two new models were generated with orientations $[0/90°]_{24}$ and $[\pm45°]_{24}$. It was assumed that the through-thickness compressive stiffness and interface friction was independent of orientation, with the only varying parameter being the orientation of the fibres in each layer.

In all cases, the compaction of the laminate on to the tool results in excess length, as the geometry, compressibility, loading and surface interactions are the same in each model. Due to the differing lay-ups, however, the excess length in each model is accommodated through different deformation mechanisms. The thickness variation of the compacted models, in Fig. 12b, show that in each configuration the presence of the radius causes some non-linearity in thickness around the corner region. While the variation between the baseline case and $[\pm45°]_{24}$ stack is minimal, the $[0/90°]_{24}$ differs greatly.

For the $[\pm45°]_{24}$ and baseline case, the wrinkle magnitude in the centre of the radius is very similar, however, the surface appears to undulate more in the web and flange of the $[\pm45°]_{24}$ model. The $[0/90°]_{24}$ result differs considerably from the other lay-ups, showing only a slight increase in thickness around the radius. As the 0/90° has more fibres oriented around the profile of the tool, there is a

higher flexural stiffness in the material to resist out-of-plane buckling, suppressing out-of-plane fibre misalignment. However, it is evident in Fig. 13 that large in-plane shear deformation appears in this region which is not present in the baseline or $[\pm45°]_{24}$ models, suggesting the length is absorbed predominantly through in-plane buckling of the fibre as the shear angle fluctuates between positive and negative values. Such phenomena have been observed experimentally in [24]. Though it should be highlighted that the current modelling approach does not include in-plane bending stiffness that would resist drastic changes in shear angle.

7.3. Tool radius

The studies have, so far, shown that the excess length is typically confined to the radius. From Eq. (1), it is apparent that the excess length is independent of the size of tool radii, however it does effect the space available for the excess length to be accommodated over as well as the geometric boundary conditions. Three different radii have been examined and compared: 5 mm, 10 mm and 20 mm.

The average thickness around the profile of the tool is presented in Fig. 12c. In each case the excess material is accommodated through out-of-plane wrinkles confined to the corner region. As the radius is increased, multiple wrinkles with lower magnitude are generated. This is likely due to the bending length of the material changing between the different radii. The change in topology of the surface appears to reduce the thickness of the part both in the web and flange region.

7.4. Arm length

The effect of arm length has been discussed in a number of studies. The hypothesis is that with increased arm length the frictional force is increased. This, subsequently, inhibits the dispersion of the excess length at the end of the laminate through inter-ply shear. Belnoue et al. [19] found that the introduction of even small frictional forces can hinder this behaviour and subsequently cause wrinkles. The results shown in Fig. 12d lead to a similar conclusion. Even small arm lengths (i.e. 25 mm) induces wrinkles and, in this case, the amplitude of the wrinkle is even increased. This could be a product of the bag configuration, as the bag is constrained to move only radially to the centre of the tool, causing the bag to pinch the laminate and draw it towards the centre of the radius. As there is less frictional resistance, the bag is able to draw in more material.

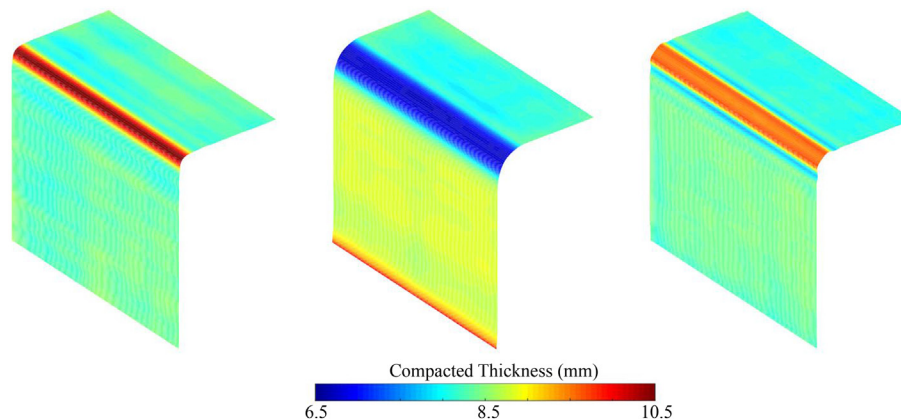Compacted Thickness (mm)

6.5   8.5   10.5

Fig. 11. Gradient plots showing variation of thickness - comparison of models with different pressure distributions, conformal bag (left), bridging bag (centre) and hydrostatic pressure (right).
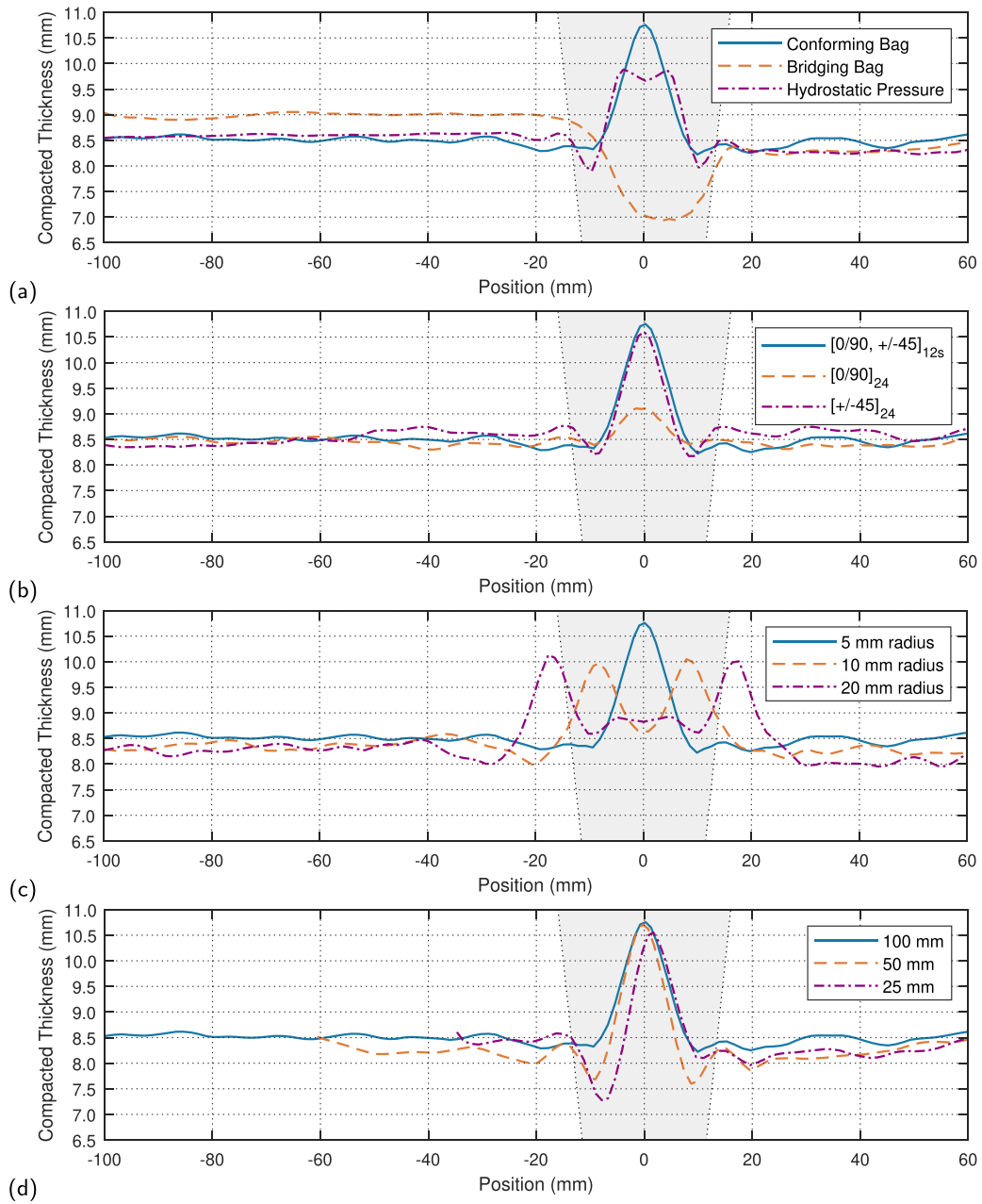
Fig. 12. Average thickness variation around profile of tool with the radius region highlighted in grey, the negative positions represent the thickness along the flange and the positive position values are the web - comparisons of models with (a) different pressure distributions (b) different fibre orientations (c) different tool radii (d) different flange/arm lengths.
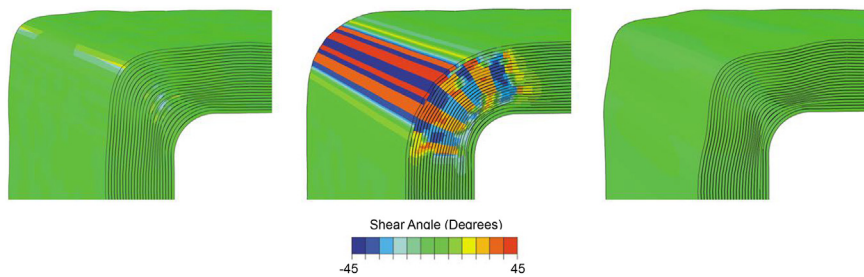

Fig. 13. In-plane shear distribution of model highlighting the presence of in-plane fibre waviness, [0/90° ±45°]$_{12s}$ baseline case (left), [0/90]$_{24}$ (centre), [±45]$_{24}$ (right).

8. Conclusions

Process modelling of textile composites has, to date, focused primarily on the forming of the planar materials into three dimensional shapes. The process typically induces large shear strains in the plane of the material, which is considered to be the main driving mechanism for wrinkles. As such, few models have been presented that focus on predicting consolidation-induced defects. Although the magnitude of these deformations is often smaller, their presence can still have detrimental effects on the performance of the final component, especially in critical regions such as corner radii. A numerical approach has, therefore, been developed to include the non-linear through-thickness compliance of textiles into a modelling approach designed for forming simulations. This method allows for the through-thickness compliance of the material to be captured through surface interactions, rather than the material behaviour, by adapting the pressure-overclosure relationship of the penalty contact.

The predictive capability of the method has been shown through comparisons with experimental trials where wrinkle defects were formed. The simulations were able to predict both the location, shape and magnitude of the wrinkle. The model was further used to assess the influence that various design parameters have on the severity of wrinkles. The configuration of the vacuum bag was shown to significantly modify the morphology of the compacted lay-up, with excess bagging material encouraging wrinkle formation and insufficient bagging material producing notable thinning in the region of the radius.

The fibre orientation, with respect to the profile of the tool, also showed to significantly alter the topology of the compacted lay-up. When the dominant fibre direction is aligned with the tool profile, the higher flexural stiffness along the fibre path appeared to suppress out-of-plane deformation and instead, encourage in-plane buckling of the fibre path to occur. With the introduction of off-axis layers to the lay-up, instability was introduced and this instigated large out-of-plane deformation.

The method presented offers a new approach to include the through-thickness compaction behaviour into conventional textile forming models. By applying the compaction behaviour directly to the contact formulation, it is fully separated from the material definition and so can easily be applied to different approaches for modelling the fabric forming behaviour, or adapted for other classes of materials such as uni-directional prepregs. The main benefit of this approach is the ability to simulate, a wide range of conditions, making it possible to examine the effect that different parameters within the design space and manufacturing capabilities have on the final part. Through this, a better understanding of the mechanisms behind compaction induced defects can be gained and used to help inform part design and manufacturing process. This is particularly important as, currently, many of apparent defects seen in industrially-produced parts are a result of design decisions, not manufacturing anomalies [31]. Using process modelling tools, such as the one presented here, therefore provide an opportunity to mitigate against many fibre path defects currently observed due to a lack of understanding of the influential parameters at play and there interactions.

Declaration of Competing Interest

The authors declare that they have no known competing financial interests or personal relationships that could have appeared to influence the work reported in this paper.

Acknowledgements

References

[1] K. Potter, Understanding the origins of defects and variability in composites manufacture, International conference on composite materials (ICCM)-17, Edinburgh, UK 2009, pp. 18–25.

[2] K. Potter, B. Khan, M. Wisnom, T. Bell, J. Stevens, Variability, fibre waviness and misalignment in the determination of the properties of composite materials and structures, Compos. A: Appl. Sci. Manuf. 39 (9) (2008) 1343–1354.

[3] S. Mukhopadhyay, M.I. Jones, S.R. Hallett, Tensile failure of laminates containing an embedded wrinkle; numerical and experimental study, Compos. A: Appl. Sci. Manuf. 77 (2015) 219–228.

[4] S. Mukhopadhyay, M.I. Jones, S.R. Hallett, Compressive failure of laminates containing an embedded wrinkle; experimental and numerical study, Compos. A: Appl. Sci. Manuf. 73 (2015) 132–142.

[5] B. Varkonyi, J.P.H. Belnoue, J. Kratz, S.R. Hallett, Predicting consolidation-induced wrinkles and their effects on composites structural performance, Int. J. Mater. Form. (2019) https://doi.org/10.1007/s12289-019-01514-2.

[6] P. Harrison, Modelling the forming mechanics of engineering fabrics using a mutually constrained pantographic beam and membrane mesh, Compos. A: Appl. Sci. Manuf. 81 (2016) 145–157.

[7] G. Barbagallo, A. Madeo, I. Azehaf, I. Giorgio, F. Morestin, P. Boisse, Bias extension test on an unbalanced woven composite reinforcement: experiments and modeling via a second-gradient continuum approach, J. Compos. Mater. 51 (2) (2016) 153–170.

[8] N. Hamila, P. Boisse, F. Sabourin, M. Brunet, A semi-discrete shell finite element for textile composite reinforcement forming simulation, Int. J. Numer. Methods Eng. 79 (12) (2009) 1443–1466.

[9] R.H.W. ten Thije, R. Akkerman, A multi-layer triangular membrane finite element for the forming simulation of laminated composites, Compos. A: Appl. Sci. Manuf. 40 (6) (2009) 739–753.

[10] M. Komeili, A.S. Milani, On effect of shear-tension coupling in forming simulation of woven fabric reinforcements, Compos. Part B 99 (2016) 17–29.

[11] T. Abdul Ghafour, J. Colmars, P. Boisse, The importance of taking into account behavior irreversibilities when simulating the forming of textile composite reinforcements, Compos. A: Appl. Sci. Manuf. 127 (2019).

[12] T.J. Dodwell, R. Butler, G.W. Hunt, Out-of-plane ply wrinkling defects during consolidation over an external radius, Compos. Sci. Technol. 105 (2014) 151–159.

[13] P. Potluri, T.V. Sagar, Compaction modelling of textile preforms for composite structures, Compos. Struct. 86 (1–3) (2008) 177–185.

[14] Q.T. Nguyen, E. Vidal-Salle, P. Boisse, C.H. Park, A. Saouab, J. Breard, G. Hivet, Mesoscopic scale analyses of textile composite reinforcement compaction, Compos. Part B 44 (1) (2013) 231–241.

[15] A.J. Thompson, B. El Said, D. Ivanov, J.P.H. Belnoue, S.R. Hallett, High fidelity modelling of the compression behaviour of 2d woven fabrics, Int. J. Solids Struct. 154 (2018) 104–113.

[16] P. Hubert, A. Poursartip, Aspects of the compaction of composite angle laminates: an experimental investigation, J. Compos. Mater. 35 (1) (2001) 2–26.

[17] G. Fernlund, J. Griffith, R. Courdji, A. Poursartip, Experimental and numerical study of the effect of caul-sheets on corner thinning of composite laminates, Compos. A: Appl. Sci. Manuf. 33 (3) (2002) 411–426.

[18] M. Li, C.L. Tucker III, Modeling and simulation of two-dimensional consolidation for thermoset matrix composites, Compos. A: Appl. Sci. Manuf. 33 (6) (2002) 877–892.

[19] J.P.H. Belnoue, O.J. Nixon-Pearson, A.J. Thompson, D.S. Ivanov, K.D. Potter, S.R. Hallett, Consolidation-driven defect generation in thick composite parts, J. Manuf. Sci. Eng. 140 (7) (2018).

[20] H. Xiong, N. Hamila, P. Boisse, Consolidation modeling during thermoforming of thermoplastic composite prepregs, Materials 12 (18) (2019) 2853.

[21] A. Levy, P. Hubert, Vacuum-bagged composite laminate forming processes: predicting thickness deviation in complex shapes, Compos. A: Appl. Sci. Manuf. 126 (2019) 105568.

[22] J.P.-H. Belnoue, S.R. Hallett, A rapid multi-scale design tool for the prediction of wrinkle defect formation in composite components, Mater. Des. 187 (2020) 108388.

[23] T. Gutowski, Z. Cai, S. Bauer, D. Boucher, J. Kingery, S. Wineman, Consolidation experiments for laminate composites, J. Compos. Mater. 21 (7) (1987) 650–669.

[24] J.S. Lightfoot, M.R. Wisnom, K. Potter, Defects in woven preforms: formation mechanisms and the effects of laminate design and layup protocol, Compos. A: Appl. Sci. Manuf. 51 (2013) 99–107.

[25] A.J. Thompson, J.P.-H. Belnoue, S.R. Hallett, Modelling defect formation in textiles during the double diaphragm forming process, Accepted in Compos. Part B (2020), https://doi.org/10.1016/j.compositesb.2020.108357.

[26] X.Q. Peng, J. Cao, A continuum mechanics-based non-orthogonal constitutive model for woven composite fabrics, Compos. A: Appl. Sci. Manuf. 36 (6) (2005) 859–874.

[27] M.A. Khan, T. Mabrouki, E. Vidal-Sallé, P. Boisse, Numerical and experimental analyses of woven composite reinforcement forming using a hypoelastic behaviour. Application to the double dome benchmark, J. Mater. Process. Technol. 210 (2) (2010) 378–388.

[28] R.S. Pierce, B.G. Falzon, M.C. Thompson, A multi-physics process model for simulating the manufacture of resin-infused composite aerostructures, Compos. Sci. Technol. 149 (2017) 269–279.

[29] H. Xiong, E.G. Maldonado, N. Hamila, P. Boisse, A prismatic solid-shell finite element based on a dkt approach with efficient calculation of through the thickness deformation, Finite Elem. Anal. Des. 151 (2018) 18–33.

[30] F. Nosrat Nezami, T. Gereke, C. Cherif, Analyses of interaction mechanisms during forming of multilayer carbon woven fabrics for composite applications, Compos. A: Appl. Sci. Manuf. 84 (2016) 406–416.

[31] K. Potter, But how can we make something useful out of black string? the development of carbon fibre composites manufacturing (1965–2015), The Structural Integrity of Carbon Fiber Composites, Springer 2017, pp. 29–57.